



Tensile strength prediction by regression analysis for pulverized glass waste-reinforced aluminium alloy 6061-T6 friction stir weldments

B T OGUNSEMI^{1,2,3}, O M ETA³, E OLANIPEKUN³, T E ABIOYE^{4,*}  and T I OGEDENGBE³

¹Landmark University SDG-9 (Industry, Innovation and Infrastructure Research Group), Omu-Aran, Kwara State, Nigeria

²Mechanical Engineering Department, College of Engineering, Landmark University, P.M.B 1001, Omu-Aran, Kwara State, Nigeria

³Mechanical Engineering Department, Federal University of Technology Akure, PMB 704, Akure, Ondo State, Nigeria

⁴Industrial and Production Engineering Department, Federal University of Technology Akure, PMB 704, Akure, Ondo State, Nigeria
e-mail: teabioye@futa.edu.ng

MS received 21 July 2021; revised 23 December 2021; accepted 5 January 2022

Abstract. AA6061-T6 is becoming a material of choice in the automobile, marine and aerospace industries because of its combination of relatively favourable and superior properties including high toughness, strength and excellent corrosion resistance. The major issue of concern about this material is the deterioration of these properties in the welded joint which has been established to improve through the additions of synthetic reinforcements such as SiC, WC, Al₂O₃, B₄C and SiO₂. This study seeks to investigate the quality of pulverised glass waste-reinforced friction stir welded joints of AA6061-T6 within a process window (rotational speed: 900-1400 rpm; traverse speed: 25-63 mm/min; tilt angle: 1° - 2.5°) as well as developing a regression model predicting the tensile strength of the pulverised waste glass-reinforced AA6061-T6 friction stir welded joints at varying process parameters. The tensile strength of the weldment was determined using Instron universal testing machine while the model was developed using a new statistical method (analysis of variance and hierarchy rule). The effects of the interaction of the parameters on the joint quality were also determined. Optimum tensile strength of ~185 MPa was achieved at rotational speed of 1120 rpm, traverse speed of 40 mm/min and tilt angle of 1.5°. There is an improvement of about 37% over the unreinforced joint with tensile strength of ~135 MPa. A model with a prediction accuracy of 92% was developed. The analysis of variance revealed that tool rotational speed, traverse speed and tilt angle had significant effects on the tensile strength of the weldments while the factors' interactions do not show any significant contribution to the tensile strength. The model finds technical applications where timely selection of optimum process parameters is required for producing particulate-reinforced AA6061-T6 friction stir welded joints.

Keywords. Aluminium alloy 6061-T6; friction stir welding; regression model; pulverised glass waste reinforcement; Tensile strength; Analysis of variance.

1. Introduction

The modern drive for the manufacture of high fuel economy and high-speed automobiles and aircrafts has forced manufacturers in the automotive and aerospace industries to seek materials with high strength to weight ratio, good ductility, excellent corrosion resistance and low cost. Since aluminium alloys have excellent combination of these properties, they have become the materials of choice extensively utilized for parts making in these industries [1, 2]. Specifically, AA6061-T6 (heat-treated) is utilised for

the making of structural parts such as car body frame and rims, aircraft wings and fuselages because of its high toughness and high strength [3–5]. AA6061-T6 is a heat-treatable, precipitation hardened aluminium-magnesium-silicon (Al-Mg-Si) alloy.

Most of the times, large engineering components are not fabricated in a single process. Joining of parts which is often achieved via welding may be required [6]. Also, repair of defective parts sometimes warrants welding operations. Welding of aluminium alloys using fusion welding techniques has been challenging because of the excessive heat involved leading to vapourization of the alloying elements such as Si and Mg from the weld pool

*For correspondence

[4]. This results in the deterioration of the weld quality [7, 8]. Other challenges associated with the fusion welding of aluminium alloys include distortion, high tendency for solidification cracks, porosity and vapourization of principal alloying elements which culminates into loss of joint strength [9]. In a bid to mitigate these challenges, friction stir welding (FSW) technology was developed [10–12]. FSW was invented by Wayne Thomas at The Welding Institute (TWI) Cambridge, UK in 1991. This welding technique has been effectively applied for joining metallic alloys and composites with great potentials in manufacturing industries. In FSW, two or more similar or dissimilar metallic materials or composites are intermixed mechanically and plastically deformed under mechanical pressure and elevated temperatures [13]. Though FSW has been established to be suitable for joining aluminium alloys [14], there is difficulty in the production of high-quality sound welds of AA6061-T6. The reason being that AA6061-T6 loses its structural strength at temperatures beyond 250°C due to the dissolution of the strengthening precipitates (B''-Mg₅Si₆) [15].

According to Ogunsemi *et al* [3], several efforts have been geared towards improving the mechanical properties of friction stir welded (FSWed) joints of AA6061-T6. The major ones among these are parametric optimization of FSW process and addition of nano and micro-sized particles as reinforcements which have shown significant improvements in the weld quality [16–20]. So far, the use of nano and micro-sized synthetic ceramic powders which include SiC, B₄C, Al₂O₃, and SiO₂ as reinforcements has been in vogue. Devaraju *et al* [21] (SiC, Al₂O₃), Jafari *et al* [22] (SiO₂), Singh *et al* [23] (TiO₂, TiC Al₂O₃), Abioye *et al* [20] (SiC, B₄C, Al₂O₃) and Nikoo *et al* [24] (Al₂O₃) have reported the effect of conventional reinforcement particles on the microstructure, mechanical and wear properties of AA6061-T6 friction stir welded joints. Their studies revealed that the utilization of synthetic powders as reinforcements showed significant improvement on the unreinforced joint in terms of the microstructure, mechanical and tribological properties of AA6061-T6 friction stir weldments. However, procuring these synthetic powders or ceramics is expensive and can be sometimes challenging [25]. Alternatively, researchers have adopted the use of non-crystalline or amorphous powders, such as copper powder [26, 27], graphite, carbon nanotubes and graphene [28] as potential and cost-effective replacements for the conventional synthetic particles. Till date, the use of

amorphous particles as reinforcement for FSW of aluminium alloys especially AA6061-T6, is still scanty. The utilization of agricultural and industrial ceramic wastes is increasingly gaining attention as an alternative reinforcement in the FSW of AA6061-T6. For example, Hussain *et al* [29] and Pradeepraj and Tamilamudhan [30] have utilized amorphous silica particles obtained from rice husk ash as reinforcements for friction stir welding of 6061-T6 aluminium alloy. The results showed that hard silica particles restricted the grain growth (pinning effect and grain refinement) of the aluminium matrix in the stir zone which led to a significant improvement in the mechanical properties of the aluminium matrix in AA6061-T6 friction stir welded joints. So far, little or no work has been reported on the use of pulverised glass wastes as reinforcement in AA6061-T6 friction stir welded joints. Glass particles (especially the borosilicate glass family) are hard amorphous ceramics with density of 2.23 g/cm³, melting point of 820 °C and hardness of 580 HV [31]. Borosilicate glass constitutes over 80% silica (SiO₂) as its principal element. In this work, the weld quality of PGW-reinforced AA6061-T6 friction stir weldments was investigated. Thereafter, a linear regression model predicting the tensile strength (TS) of the weldments was developed and validated.

2. Experimental

2.1 Materials

6 mm thick rolled plates of precipitation hardened AA6061-T6 supplied by Aluminum Rolling Mill Coy., Malaysia, was utilized as the workpiece. The chemical composition of the material, as obtained via X-ray fluorescence (XRF) analysis, is presented in table 1. Plates of dimension 100 × 50 × 6 mm were machined and prepared prior to FSW process. A butt joint configuration having a centre groove of dimension 94 × 2 × 4.5 mm (L × B × H) along the weld-line was prepared. The groove was then manually filled with pulverised glass waste (PGW) and then closed up by ensuring a single pass of a rotational pin-less tool over it. The pinless tool has a shoulder of 20 mm. This was carried out to prevent the glass powder from being dispersed or scattered during FSW. PGW of <45 μm size was utilized as reinforcement particles in this work. The elemental analysis of the PGW, as determined by energy-dispersive X-ray (EDX) analysis, is presented in figure 1.

Table 1. Chemical composition of the AA6061-T6 plate as determined by XRF analysis.

Elements	Mg	Si	Fe	Cu	Mn	Cr	Ni	Zn	Ti	Al
Wt. (%)	0.891	0.562	0.314	0.265	0.039	0.231	0.014	0.053	0.019	Bal

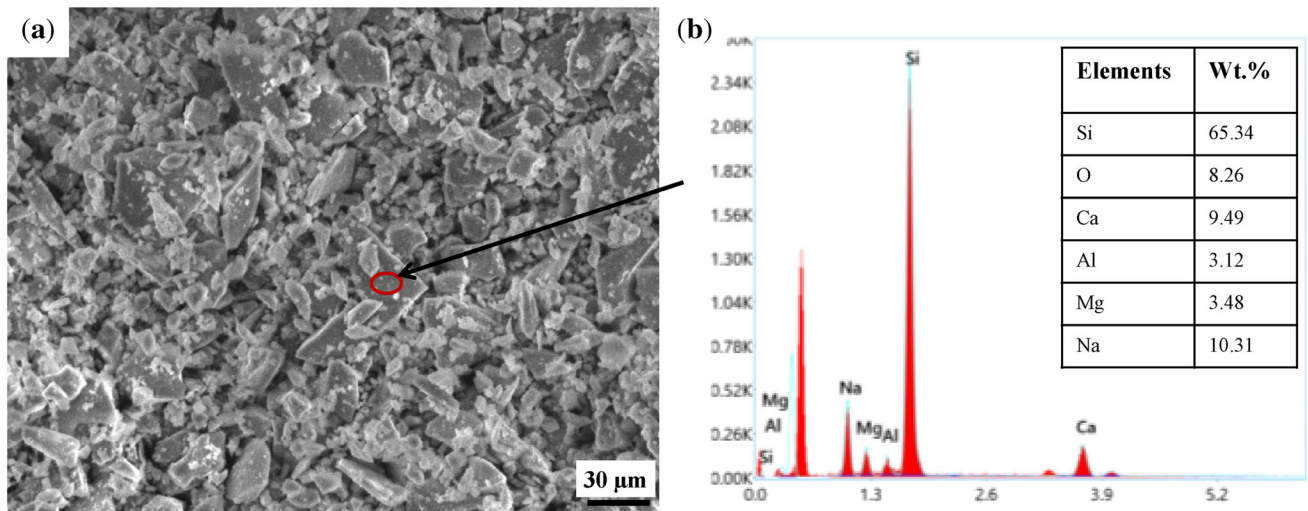


Figure 1. (a) SEM Micrograph of the pulverised glass powder. (b) EDS analysis showing the various elemental compositions.

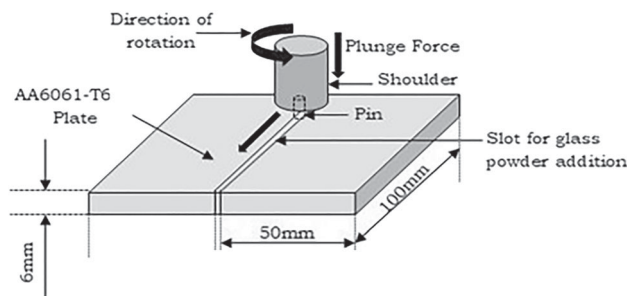


Figure 2. Schematic diagram of friction stir welding process.

2.2 Friction stir welding

The schematic of the FSW process is illustrated in figure 2. A non-consumable rotating high-speed steel (HSS) tool with pin was integrated with the vertical milling machine and used to fabricate the joints via a single pass FSW process. The tool shoulder is of diameter 20 mm while the tool pin (tapered) is of diameter 4.5 - 4 mm from the shoulder over a length of 4.5 mm. FSW with butt joint configuration was performed using full factorial experimental design with three factors and three levels (3^3 matrix). The factors include tool rotational speed (rpm), traverse speed (mm/min) and tilt angle (degrees). Design of Experiment was carried out to randomize the parametric combination as presented in tables 2 and 3. Twenty-seven (27) experimental runs were obtained from 3^3 factorial experimental design. As shown in table 3, the standard order was randomized to avoid systematic error. Each experimental run was repeated three times to produce three (3) test samples under the same welding condition in order to account for statistical errors and experimental uncertainties during analysis.

2.3 Tensile strength test

Test specimens for the tensile strength were machined and prepared based on the ASTM-E8M-13 standard (see figure 3). The tensile test was carried out using Instron 3369 universal tensile testing machine. Tensile tests were done using the x-head velocity or loading rate of 5 mm/min. Three (3) specimens were prepared and tested for each experimental run so as to obtain the average value of the three measurements, thereby enhancing the reliability of the results obtained.

2.4 Regression model analysis

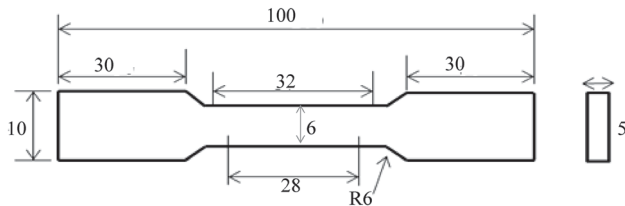
The results of both the tensile and hardness tests obtained in this study were used to generate mathematical models using analysis of variance (ANOVA) and regression analysis. These were carried out to establish a linear relationship (mathematical model) between the tensile strength of friction stir welded (FSWed) joints of AA6061-T6 and the welding parameters considered. Minitab 17 software was used to perform the analyses. The significance of the factors and their interactions was determined via the use of ANOVA (95% confidence level). The three-way interactions of parameters (with P values > 0.05) was first

Table 2. Process conditions for friction stir welding of AA6061-T6.

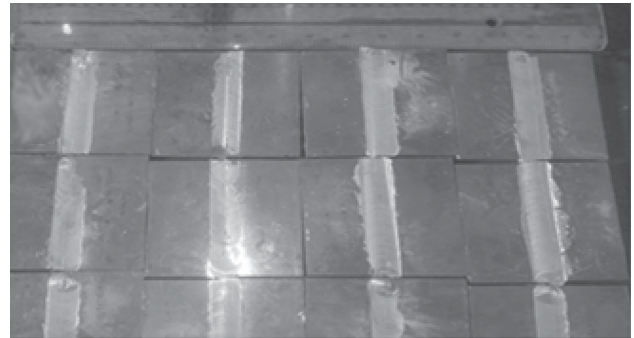
Levels (n)	Rotational speed (rpm)	Travel speed (mm/min)	Tilt angle (degrees)
1	900	25	1
2	1120	40	1.5
3	1400	63	2.5

Table 3. Full factorial design of experiment (DoE) for parametric optimization.

Std. order	Run order	Rotational speed (rpm)	Travel speed (mm/min)	Tilt angle (°)
23	1	900	25	2.5
19	2	1400	40	1.5
4	3	900	25	1.5
5	4	1400	63	1.5
24	5	900	40	1.5
14	6	1400	25	1.5
10	7	900	40	2.5
20	8	1120	40	1.5
25	9	1120	40	2.5
21	10	900	40	1
17	11	1120	25	2.5
9	12	1400	25	1
8	13	1120	40	1
27	14	1120	63	1
12	15	1120	25	1
22	16	1120	63	1.5
1	17	1120	25	1.5
13	18	1400	40	2.5
7	19	900	63	2.5
11	20	1400	25	2.5
15	21	1400	63	1
3	22	900	63	1
2	23	1400	63	2.5
18	24	1120	63	2.5
16	25	1400	40	1
26	26	900	63	1.5
6	27	900	25	1

**Figure 3.** Schematic diagram of a tensile test specimen (all dimensions in mm).

performed on the measured values of the tensile strength. The non-significant factors and interactions (having P value above 0.05) were eliminated in order to come up with a valid model for the data. In order to refine the model, hierarchy rule was adopted to strategically remove non-significant factors and interactions starting from the three-way interaction. Subsequently, interactions or factors with P value above 0.05 were removed first before the single factors were eliminated from the model based on their P value variance from 0.05. Hence, regression analysis was

**Figure 4.** Some selected pulverised glass waste-reinforced AA6061-T6 friction stir weldments.

carried out in order to generate mathematical equations that connect the significant factors with the responses. Contour plots were also generated to show the relationship between two continuous parameters and a fitted response in two dimensions. The developed model is validated by performing confirmatory tests on the tensile strength.

3. Results and discussion

3.1 Visual observation of the weldments

Figure 4 presents some of the selected friction stir weldments produced during the optimization process. The surfaces of the joints are free of visible defects such as cracks and pores. The absence of these surface defects is an indication that the range of parameters selected for this work is appropriate. Also, good visual surface integrity exhibited by the weldments shows that the PGW particles (i.e. reinforcement) were properly intermixed and bonded with the AA6061-T6 matrix.

3.2 Experimental (measured) values of the tensile strength

The results of the tensile strength obtained from the 27 experimental runs conducted are presented in table 4. The range of tensile strength for the friction stir weldments is between 127.2 and 185.1 MPa. Tensile strength of 127.2 MPa was produced at welding conditions of 900 rpm, 25 mm/min, 1° while 185.1 MPa (maximum value) was achieved at 1120 rpm, 40 mm/min, 1.5° respectively.

The main effect plot showing the variation of the tensile strength with rotational speed, traverse speed and tilt angle is presented in figure 5. It is evident from the main effect plot that the tensile strength increased as the rotational speed increased from 900 rpm to 1120 rpm and then decreased as the rotational speed increased further to 1400 rpm. Also, the tensile strength first increased as the traverse speed increased from 25 to 40 rpm and then decreased with further rise in traverse speed to 63 mm/min. The explanation for these trends can be attributed to (i) effect of dynamic recrystallization and pinning causing enhanced grain refinement and (ii) the loss of the structural strengthening at higher heat input causing softening of the welded joint.

At a reduced rotational speed of 900 rpm, the stirring action of the rotating tool could not generate substantial amount of frictional heat energy sufficiently required to cause severe plastic deformation of the aluminium matrix. Consequently, as revealed in figure 5, the tensile strength at this speed is low. According Klog *et al* [7], low stirring action would not produce substantial grain refinement due to low degree of plastic deformation. As the rotational speed increased from 900 to 1120 rpm, the increased stirring action resulted in more severe plastic deformation and higher degree of dynamic recrystallization [7, 9]. Hence,

Table 4. Results of the experimental tensile test.

Run order	Rotational speed (rpm)	Traverse speed (mm/min)	Tilt angle (degrees)	Tensile strength (MPa)
1	900	25	2.5	141.69
2	1400	40	1.5	168.488
3	900	25	1.5	147.245
4	1400	63	1.5	150.224
5	900	40	1.5	159.537
6	1400	25	1.5	149.091
7	900	40	2.5	149.396
8	1120	40	2.5	177.877
9	1120	40	1.5	185.021
10	900	40	1	143.734
11	1120	25	2.5	157.146
12	1400	25	1	142.688
13	1120	40	1	162.417
14	1120	63	1	149.889
15	1120	25	1	143.173
16	1120	63	1.5	153.527
17	1120	25	1.5	155.018
18	1400	40	2.5	158.685
19	900	63	2.5	132.714
20	1400	25	2.5	145.235
21	1400	63	1	134.016
22	900	63	1	130.678
23	1400	63	2.5	148.034
24	1120	63	2.5	172.192
25	1400	40	1	156.69
26	900	63	1.5	140.499
27	900	25	1	127.245

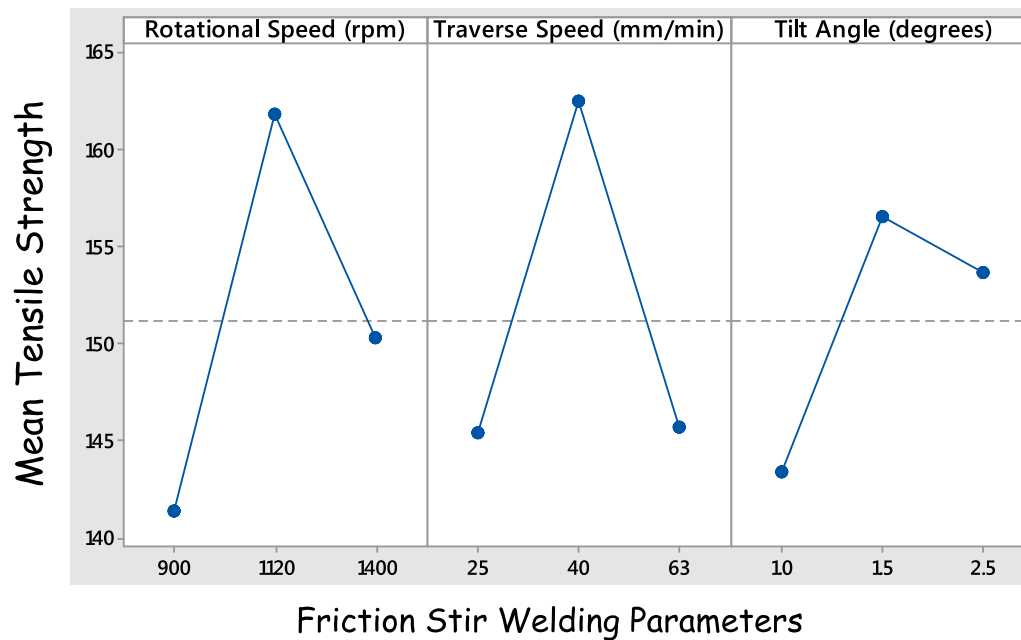


Figure 5. Main effect plot of the tensile strength of pulverised glass waste-reinforced AA6061-T6 friction stir weldment.

the substantial grain refinement resulting from increased dynamic recrystallization is believed to have suppressed the negative effect (softening resulting from loss of strengthening precipitates) of higher frictional heat generated at this speed. This was the reason for the rise in the tensile strength. Further increase in the rotational speed from 1120 to 1400 rpm generated more heat causing more dissolution of the strengthening precipitates in the AA6061-T6. Though the increased rotational speed caused more plastic deformation and improved grain refinement, the increased heat generated leading to dissolution of the main strengthening precipitates is believed to have more effect on the joint at this condition [32]. As a result, a decrease in the tensile strength was discovered as the rotational speed increased beyond 1120 rpm.

At low traverse speed (25 mm/min), the tool interacted longer with a unit length of the workpiece. Therefore, there was increased localised heating which is believed to have caused higher loss of the structural strengthening (T6-condition) in the aluminium alloy [3]. Hence, low tensile strength was found at this value of traverse speed. However, as the traverse speed increased to 40 mm/min, the tool interaction time per unit length of weld decreased causing reduction in the localised heating and reduced dissolution of the strengthening precipitates. Consequently, the tensile strength improved. Further increase in the traverse speed to 63 mm/min did not generate sufficient localised heating because the tool interaction with a unit length of the workpiece was too fast. A very strong bond or joint was not produced at this condition and the tensile strength declined.

As shown in figure 5, the tensile strength improved as the tilt angle increased from 1° to 1.5°. Thereafter, the tensile strength started to decline. This finding is similar to that of Zhao *et al* [18] and Jafari *et al* [22] who established that high quality joint of AA6061-T6 can be achieved at tilt angles ranging between 1.5° and 2.5°. According to Banik *et al* [19], increasing the tilt angle from 1 to 3° results in the accumulation of more materials under the tool shoulder as the tool traverses. The implication of this is that there is better mixing of materials and creation of larger material flow zone which enhances the hardness and tensile strength of the welded joint. However, it has been otherwise proved that too high tilt angle brings about weld thinning which is a flaw in FSW that reduces the strength of the joints [3].

The maximum tensile strength of ~185 MPa was found at optimized welding conditions of 1120 rpm, 40 mm/min and 1.5°. This finding is in consistence with the work of Gharavi *et al* [17] that earlier established traverse speed of 40 mm/min as optimal for obtaining high quality AA6061-T6 friction stir weldment.

In this work, the addition of PGW to the joint resulted in improved tensile strength when compared with that of the unreinforced joint (~135 MPa). The exceptions to this occur at some few processing parameters when the combination of both rotational speed and the traverse speed could not produce sufficient plastic deformation to generate a strong bond. The maximum tensile strength of ~185 MPa was produced at optimal condition (1120 rpm rotational speed, 40 mm/min traverse speed, 1.5° tilt angle). This was about a factor of 1.4 greater than that of the unreinforced joint. The interpretation of this is that

the addition of PGW to the joint enhanced the tensile strength. It has been established in the past that the incorporation of nano or micro-sized reinforcement particles into the weld pool brings about pinning effect which often leads to increased refinement of the plastically deformed aluminium matrix during FSW [32, 33]. The reinforcement particle addition often acts as obstacles or restrictions against the growth of new grains. This phenomenon is called pinning effect and it enhances grain refinement [32, 33]. The increased tensile strength obtained for the PGW- reinforced joint can be traced to the combined effects of the dynamic recrystallisation and pinning of the grain growth by the hard particles (i.e., reinforcement).

3.3 Development of linear regression model

ANOVA and hierarchy rule was applied to the result of the tensile strength presented in table 4. As a result, a regression model predicting the tensile strength of PGW-reinforced AA6061-T6 friction stir weldment at varying process parameters was developed. First, ANOVA involving all the possible two-way interactions of the parameters utilized was performed on the experimental (measured) tensile strength values, as given in table 5. A statistical confidence level of 95% was used in this study. This implies that factors or interaction whose P-value is above 0.005 is considered insignificant. The first model, as presented in table 5, has a P value of 2.262 which is greater than 0.005. Also, the difference between the R_{sq} (87.97%) and R_{sq} (adjusted) (81.59%) values is 6.38%. The interpretation of this is that the model is not fit. Therefore, it was refined using the hierarchy rule by eliminating the most insignificant factors starting from the two-way interactions of factors. Based on the hierarchy rule, the interactions RS*TS, RS*TA and TS*TA

were removed being the most insignificant. table 6 was generated after the first refinement and the P value of the model reduced to 1.412 (still insignificant). The difference between the R_{sq} and R_{sq} (adjusted) values was also reduced to 5.36%.

Hierarchy rule was further used to refine the model (see table 7) until a model of P value of 0.002 (< 0.005) was found (see table 8). Also, the result in table 8 indicates that the model terms including RS, TS, TA, RS^2 , TS^2 , and TA^2 have the significant effect on the response (i.e. tensile strength). At this point, the difference between the R_{sq} and R_{sq} (adjusted) values reduced to 3.69%. This depicts a better fitness of model to the response (tensile strength). Furthermore, the R^2 value for the most refined model shows that 87.70% of the data variation was explained by the model, thereby validating the high reliability of the developed model. The generated coefficients used for the linear regression model development are presented in table 9. The linear regression mathematical model generated to estimate the tensile strength of PGW-reinforced AA6061-T6 friction stir weldments is given in Eq. (1). It can be deduced from the linear regression model that the model terms such as the rotational speed (RS), traverse speed (TS) and tilt angle (TA) have positive impact on the tensile strength.

$$TS = -352.9 + 0.6324RS + 4.318TS + 67.9TA - 0.000267RS^2 - 0.04896TS^2 - 17.28TA^2 \quad (1)$$

The adequacy of the model was verified by analysing residual plots as presented in figure 6. It is deduced from the normal probability plot (figure 6a) that the errors are spread or distributed normally. This is due to the fact that the residuals (i.e. data points) are distributed along the straight line. The assumption that the residuals are normally distributed is thus satisfied based on the

Table 5. ANOVA result for the two-way interaction model.

Source	DOF	Adj. SS	Adj. MS	F-value	P value
Model	9	6708.5	6708.5	188.30	2.262
Rotational Speed (RS)	1	1606.35	1606.35	45.09	0.000
Traverse Speed (TS)	1	987.03	987.03	27.70	0.000
Tilt Angle (TA)	1	364.46	364.46	10.23	0.005
Two-way interaction: RS*RS	1	1617.83	1617.83	45.41	0.000
Two-way interaction: TS*TS	1	1687.25	1687.25	47.36	0.000
Two-way interaction: TA*TA	1	432.14	432.14	12.13	0.003
Two-way interaction: RS*TS	1	1.64	1.64	0.050	0.833
Two-way interaction: RS*TA	1	2.06	2.06	0.06	0.813
Two-way interaction: TS*TA	1	9.74	9.74	0.27	0.608
Error	17	605.69	35.63		
Total	26	5033.11			

R-sq = 87.97%; R-sq (adj) = 81.59%; R-Sq(pred) = 68.51%

Table 6. ANOVA result for the refined two-way interaction model.

Source	DOF	Adj. SS	Adj.MS	F-value	P value
Model	8	7196.16	7196.2	213.28	1.412
Rotational Speed (RS)	1	1667.19	1667.2	49.41	0.000
Traverse Speed (TS)	1	1415.49	1415.5	41.95	0.000
Tilt Angle (TA)	1	364.46	364.46	10.80	0.004
Two-way interaction: RS*RS	1	1617.83	1617.8	47.95	0.000
Two-way interaction: TS*TS	1	1687.25	1687.3	50.01	0.000
Two-way interaction: TA*TA	1	432.1	432.14	12.81	0.002
Two-way interaction: RS*TA	1	2.06	2.06	0.06	0.808
Two-way interaction: TS*TA	1	9.74	9.74	0.29	0.598
Error	18	607.33	33.74		
Total	26	5033.11			

R-sq = 87.93%; R-sq (adj) = 82.57%; R-sq(pred) = 71.65%

Table 7. ANOVA result for the refined two-way interaction model.

Source	DOF	Adj. SS	Adj.MS	F-value	P value
Model	7	7297.18	7297.18	227.51	0.591
Rotational Speed (RS)	1	1692.4	1692.4	52.77	0.000
Traverse Speed (TS)	1	1415.49	1415.49	44.13	0.000
Tilt Angle (TA)	1	442.33	442.33	13.79	0.001
Two-way interaction: RS*RS	1	1617.83	1617.83	50.44	0.000
Two-way interaction: TS*TS	1	1687.25	1687.25	52.61	0.000
Two-way interaction: TA*TA	1	432.14	432.14	13.47	0.002
Two-way interaction: TS*TA	1	9.74	9.74	0.30	0.588
Error	19	609.39	32.07		
Total	26	5033.11			

R-sq = 87.89%; R-sq (adj) = 83.43%; R-sq (pred) = 74.45%

Table 8. ANOVA result for the refined two-way interaction model.

Source	DOF	Adj. SS	Adj.MS	F-value	P value
Model	6	7572	7572.01	244.6	0.002
Rotational Speed (RS)	1	1692.4	1692.4	54.67	0.000
Traverse Speed (TS)	1	1625.6	1625.6	52.51	0.000
Tilt Angle (TA)	1	516.8	516.83	16.7	0.001
Two-way interaction: RS*RS	1	1617.8	1617.8	52.26	0.000
Two-way interaction: TS*TS	1	1687.3	1687.3	54.5	0.000
Two-way interaction: TA*TA	1	432.1	432.14	13.96	0.001
Error	20	619.1	30.96		
Total	26	5033.1			

R-sq = 87.70%; R-sq (adj) = 84.01%; R-sq (pred)=77.58%

Table 9. Coefficients of the refined two-way interaction model.

Term	Coefficient	SE coefficient	P value
Constant	− 352.9	51.3	0.000
RS	0.6324	0.0855	0.000
TS	4.318	0.596	0.000
TA	67.9	16.6	0.001
RS ² (RA*RA)	− 0.000267	0.000037	0.000
TS ² (TS*TS)	− 0.04896	0.00663	0.000
TA ² (TA*TA)	− 17.28	4.63	0.001

previous study conducted by Abioye *et al* [20]. The model was further verified by carrying out the versus fits and versus order plots. It is apparent from figure 6b that the residuals seem to be randomly distributed across the high and low fitted values. This depicts that the assumption of the regression model was satisfied across a

range of fitted values. The random and uneven pattern in figure 6b shows that the residuals have non-constant variance [34]. The versus order plot in figure 6c also describes the random pattern of the residuals. This plot illustrates that the linear regression model is adequately fit to predict the output response.

3.4 Validation of the model

The predicted tensile strength values for all the 27 experimental runs were calculated and compared with the measured experimental values. As clearly shown in table 10, the deviations of the predicted tensile strength values from the experimental values for the entire 27 experimental runs are less than 8%. This indicates that the linear model can predict to an accuracy of 92%. This measure of accuracy is similar to that obtained by Abioye *et al* [35] on the prediction modelling of the tensile strength values of AA5052-H32 fibre laser welding.

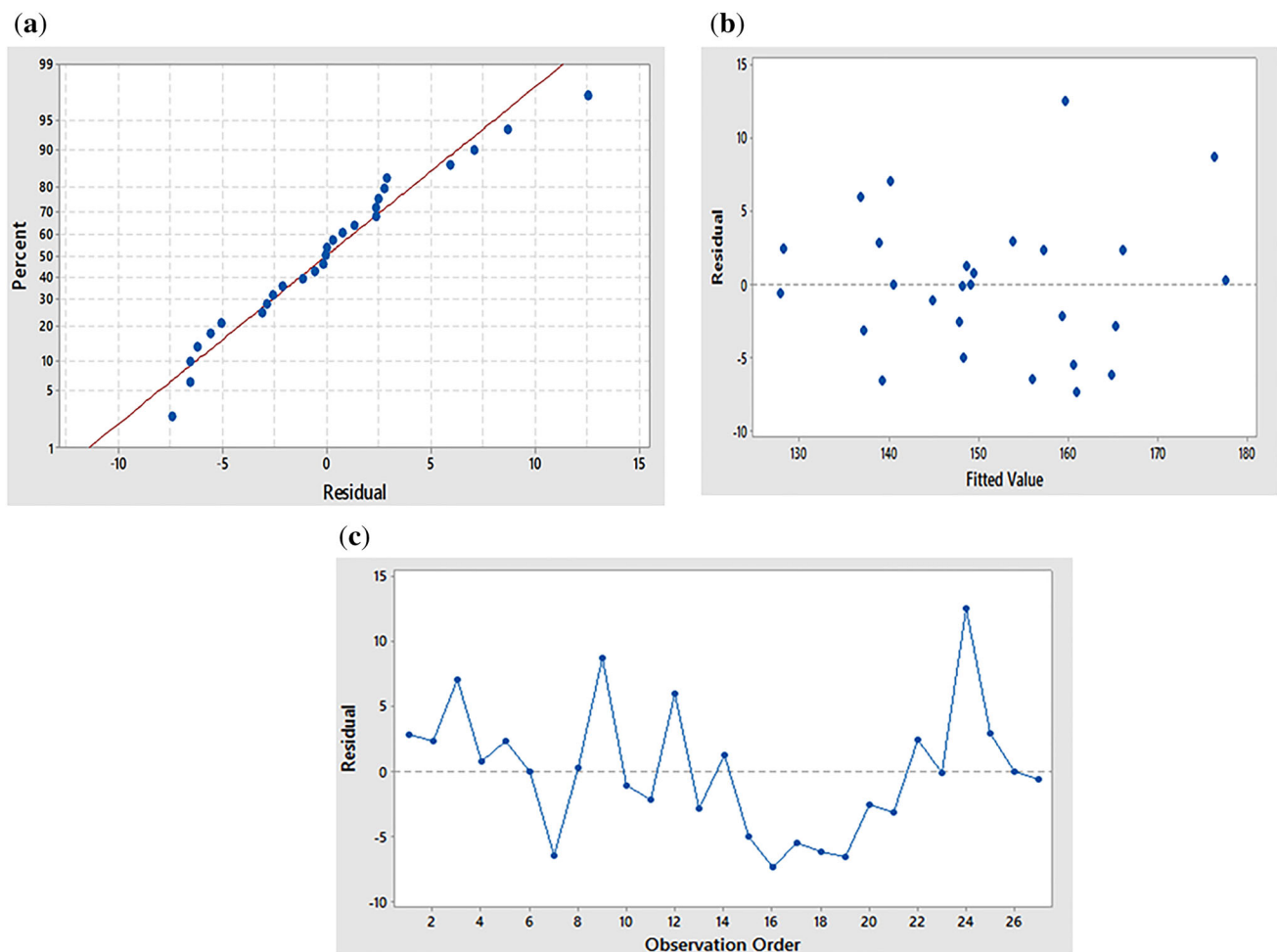


Figure 6. Residual plots showing the model fitness for (a) normal probability, (b) versus fit and (c) versus order.

Table 10. Variations between the measured and predicted values of the tensile strength.

Run order	Process parameters			Tensile strength (MPa)		Difference (%)
	Rotational speed (rpm)	Traverse speed (mm/min)	Tilt angle (degrees)	Measured experimental	Model predicted	
1	900	25	2.5	141.7	139.1	1.8
2	1400	40	1.5	168.5	166.5	1.2
3	900	25	1.5	147.2	140.3	4.7
4	1400	63	1.5	150.2	149.8	0.3
5	900	40	1.5	159.5	157.3	1.4
6	1400	25	1.5	149.1	149.5	0.2
7	900	40	2.5	149.4	156.1	4.5
8	1120	40	1.5	177.9	177.8	0.03
9	1120	40	2.5	185.0	176.6	4.6
10	900	40	1	143.7	145.0	0.9
11	1120	25	2.5	157.1	159.6	1.5
12	1400	25	1	142.7	137.1	3.9
13	1120	40	1	162.4	165.5	1.9
14	1120	63	1	149.9	148.8	0.7
15	1120	25	1	143.2	148.4	3.7
16	1120	63	1.5	153.5	161.1	5.0
17	1120	25	1.5	155.0	160.8	3.7
18	1400	40	2.5	158.7	165.3	4.2
19	900	63	2.5	132.7	139.5	5.1
20	1400	25	2.5	145.2	148.2	2.1
21	1400	63	1	134.0	137.5	2.6
22	900	63	1	130.7	128.3	1.8
23	1400	63	2.5	148.0	148.6	0.4
24	1120	63	2.5	172.2	159.9	7.1
25	1400	40	1	156.7	154.1	1.6
26	900	63	1.5	140.5	140.7	0.1
27	900	25	1	127.2	128.0	0.6

4. Conclusion

Friction stir welding of pulverised glass waste-reinforced AA6061-T6 has been successfully investigated within a range of parameters (900-1400 rpm rotational speed, 25-63 mm/min traverse speed, 1-2.5° tilt angle). The addition of pulverised glass waste as reinforcement yielded significant improvement in the tensile strength of the AA6061-T6 friction stir welded joint. Highest tensile strength of ~185 MPa was achieved at a rotational speed of 1120 rpm, traverse speed of 40 mm/min and tilt angle of 1.5°. This was found to be higher than that of the unreinforced joint obtained using similar condition by a factor of 1.4. The tensile strength of the pulverised glass waste-reinforced AA6061-T6 friction stir welded joint increased with increasing the rotational speed until a value (1120 rpm) was reached after which the tensile strength declined. Similar trend was found for the traverse speed and tilt angle. A linear regression model predicting the tensile strength of the pulverised glass waste-reinforced AA6061-T6 friction stir welded

joint up to an accuracy of 92% was successfully developed and validated. The analysis of variance revealed that all the three parameters considered in this study contributed significantly to the tensile strength of the welded joints.

Acknowledgements

The authors appreciate the technical assistance provided by Mr C.O. Abulola of the Department of Industrial and Production Engineering, Federal University of Technology Akure, Ondo State, Nigeria. Also, the statistical assistance rendered by Miss O.O. Kusoro of Industrial Mathematics Department, Federal University of Technology Akure is highly appreciated.

Declaration

Conflict of interest The authors declare that there is no conflict of interest.

References

- [1] Singh T, Tiwari S K and Shukla D K 2019 Friction stir welding of AA6061-T6: the effect of Al₂O₃ nano particles addition. *Results in Materials*. 1: 100005
- [2] Bodunrin M O, Alaneme K K and Chown L H 2015 A review of reinforcement philosophies: mechanical, corrosion and tribological characteristics. *J. Mater. Res. Technol.* 4: 434–451
- [3] Ogunsemi B T, Abioye T E, Ogedengbe T I and Zuhailawati H 2021 A review of various improvement strategies for joint quality of AA6061-T6 friction stir weldments. *J. Mater. Res. Technol.* 11: 1061–1089
- [4] Abioye T E, Zuhailawati H, Aizad S and Anasyida A S 2019 Geometrical, microstructural and mechanical characterisation of pulse laser welded thin sheet 5052–H32 aluminium alloy for aerospace applications. *Trans. Nonferrous Met. Soc. China*. 29: 667–679
- [5] Singh V P, Patel S K, Raryan A and Chen B K 2020 Recent research progress in solid state friction stir welding of aluminium-magnesium alloys: a critical review. *J. Mater. Res. Technol.* 9: 6217–6256
- [6] Vysotskiy I, Malopheyev S, Mironov S and Kaibyshev R 2019 Effect of pre-strain path on suppression of abnormal grain growth in friction stir welded 6061 aluminium alloy. *Mater. Sci. Eng. A* 760: 206–213
- [7] Klog O, Grobner J, Wagner G, Schmid-Fetzer R and Eifler D 2014 Microstructural and thermodynamic investigation of friction stir welded Mg/Al-joints. *Int. J. Mater. Res.* 105: 145–155
- [8] Chandran R, Ramaiyan S, Shanbhag A G and Santhanam S K V 2018 Optimization of welding parameters of friction stir lap welding of AA6061-T6 alloy. *Journal of Modern Mechanical Engineering*. 8: 31–41
- [9] Shamin M K 2017 Morphological and structural study of friction stir welded thin AA6061-T6 sheets. *Int. J. Mech. Eng.* 6: 19–24
- [10] Singh K, Singh G and Singh H 2018 Review on friction stir welding of magnesium alloys. *J. Magnes. Alloy*. 16: 339–416
- [11] Abioye T E, Zuhailawati H, Anasyida A S, Ayodeji S P and Oke P K 2021 Effects of particulate reinforcements on the hardness, impact and tensile strengths of AA6061-T6 friction stir weldments. *Proc. Inst. Mech. Eng. Pt. L J. Mater. Des. Appl.* 235: 1500–1506
- [12] Venkateswaran P and Reynolds A P 2012 Factors affecting the properties of friction stir welds between aluminium and magnesium alloys. *Mater. Sci. Eng. A* 545: 26–37
- [13] Li Y Z, Zan Y N, Wang Q Z, Xiao B L and Ma Z Y 2019 Effect of welding speed and post-weld aging on the microstructure and mechanical properties of friction stir welded B4Cp/6061Al-T6 Composites. *J. Mater. Process. Technol.* 273: 1–11
- [14] Babu K T, Kumar P K and Muthukumaran S 2014 Mechanical, metallurgical characteristics and corrosion properties of friction stir welded AA6061-T6 using commercial pure aluminum as filler plate. *Procedia Material Science*. 6: 648–656
- [15] Zhao Y, Huang X, Li Q, Huang J and Yan K 2015 Effect of friction stir processing with B4C particles on the microstructure and mechanical properties of 6061 aluminium alloy. *Int. J. Adv. Manuf. Technol.* 78: 1437–1443
- [16] Anas N M, Abioye T E, Anasyida A S, Dhindaw B K, Zuhailawati H and Ismail A 2020 Microstructure, mechanical and corrosion properties of cryorolled- AA 5052 at various solution treatment temperatures. *Mater. Res. Express*. 7: 016535
- [17] Gharavi F, Matori K A, Yunus R, Othman N K and Fadaeifarad F 2015 Corrosion behaviour of Al6061 alloy weldment produced by friction stir welding process. *J. Mater. Res. Technol.* 54: 314–322
- [18] Zhao H, Pan Q, Qin Q, Wu Y and Su X 2019 Effect of processing parameters of friction stir processing on the microstructure and mechanical properties of 6063 aluminium alloy. *Mater. Sci. Eng. A* 751: 70–79
- [19] Banik A, Barnik S R, Barma J D and Saha S C 2018 An experimental investigation of torque and force generation of varying tool tilt angles and their effects on the microstructure and mechanical properties: friction stir welding of AA6061-T6. *J. Manuf. Process*. 31: 395–404
- [20] Abioye T E, Zuhailawati H, Anasyida A S, Yahaya S A and Dhindaw B K 2019 Investigation of the microstructure, mechanical and wear properties of AA6061-T6 friction stir weldments with different particulate reinforcement's addition. *J. Mater. Res. Technol.* 8: 3917–3928
- [21] Devaraju A, Kumar A, Kumaraswamy A and Kotiveerachari B 2013 Influence of reinforcements (SiC and Al₂O₃) and rotational speed on wear and mechanical properties of aluminium alloy 6061-T6 based surface hybrid composites produced via friction stir processing. *Mater. Des.* 51: 331–341
- [22] Jafari H, Monsouri H and Honarpishe M 2019 Investigation of residual stress distribution of dissimilar Al7075-T6 and Al6061-T6 in the friction stir welding strengthened with SiO₂ nanoparticles. *J. Manuf. Process*. 43: 145–153
- [23] Singh T, Tiwari S K and Shukla D K 2020 Mechanical and microstructural characterization of friction stir welded AA6061-T6 joints reinforced with nano-sized particles. *Mater. Charact.* 159: 1–14
- [24] Nikoo M F, Nader P and Mohsen B 2015 Al₂O₃-fortified AA6061-T6 joint produced via friction stir welding: The effects of traveling speed on microstructure, mechanical and wear properties. *Proc. Inst. Mech. Eng. Pt. L J. Mater. Des. Appl.* 231: 1–10
- [25] Suraya S, Shamsuddin S, Nur N J and Yusof I 2014 Studies on Tensile Properties of Titanium Carbide (TiC) particulate composites. *Adv. Mat. Res.* 903: 151–156
- [26] Mohan V K, Shamnadh M and Sudheer A 2018 Fabrication and Characterization of friction stir welding of AA6061 using Copper powder. *Mater. Today: Proceedings*. 5: 24339–24346
- [27] Ashu G and Anirban B 2019 Influence of Cu powder on strength, failure and metallurgical characterization of single, double pass friction stir welded AA6061-AA7075 joints. *Mater. Sci. Eng. A*. 759: 661–679
- [28] Maurya R, Kumar B, Anirban S, Ramkumar J and Balani K 2016 Effects of carbonaceous reinforcements on the mechanical and tribological properties of friction stir processed Al6061 alloy. *Mater. Des.* 98: 155–166

- [29] Hussain Z, Halmy M N, Almanar I P and Dhindaw B K 2014 Friction stir processed of 6061-T6 Aluminium Alloy Reinforced with Silica from Rice Husk Ash. *Adv. Mat. Res.* 1024: 227–230
- [30] Pradeepraj A and Tamilmudhan P 2017 Effect of Rice Husk Ash and SiC Particles on hardness and microstructure of friction stir welded metal matrix composites. *International Journal for Scientific Research and Development.* 5: 1–6
- [31] Barlet M, Delaye J M, Charpentier T, Gennisson M, Bonamy D, Rouxel T and Rountree C L 2015 Hardness and toughness of Sodium borosilicate glasses via Vickers indentations. *Journal of Non-Crystalline Solids.* 417: 66–79
- [32] Abioye T E, Zuhailawati H, Anasyida A S, Yahaya S A and Faizul Hilmy M N 2021 Enhancing the Surface Quality and Tribomechanical Properties of AA6061-T6 Friction Stir Welded Joints Reinforced with Varying SiC Contents. *J. Mater. Eng. Perform.* 30: 4356–4369
- [33] Hakem M, Lebaili S, Mathieu S, Miroud D, Lebaili A and Cheniti B 2019 Effect of microstructure and precipitation phenomenon on the mechanical behaviour of AA6061-T6 aluminium alloy weld. *Int. J. Adv. Manuf. Technol.* 102: 2907–2918
- [34] Zhang H, Wang M, Zhou W, Zhang X, Zhu Z, Yu T and Yang G 2015 Microstructure-property characterization of a novel non-weld thinning friction stir welding process of aluminium alloys. *Mater. Des.* 86: 379–387
- [35] Abioye T E, Mustar N, Zuhailawati H and Suhaina I 2019 Prediction of the tensile strength of aluminium alloy 5052-H32 fibre laser weldments using regression analysis. *Int. J. Adv. Manuf. Technol.* 102: 1951–1962